

A HIGH-POWER PICOSECOND Nd:YAG/CO₂ LASER SYSTEM FOR ELECTRON GUNS, LASER ACCELERATION AND FEL*

M. Babzien, I. Ben-Zvi, J. Fischer, A.S. Fisher, K. Kusche, I.V. Pogorelsky, and T. Srinivasan-Rao
Accelerator Test Facility, Brookhaven National Laboratory, Upton, NY 11973

Abstract

Fourth-harmonic Nd:YAG pulses illuminating a microwave linear accelerator's photoinjector generates electron bunches in trains for FEL experiments, or in a single pulse for laser acceleration. A multi-gigawatt CO₂ laser switched by the Nd:YAG fundamental delivers 50-ps pulses for Inverse Cherenkov, Inverse FEL, or Grating Linac electron acceleration experiments.

I. Introduction

The Accelerator Test Facility (ATF)¹ is a users facility at BNL that provides a high brightness electron beam and high power laser pulses to study new methods of high-gradient acceleration and free electron lasers. A number of users from national laboratories, universities, and industry take part in the experimental program at the ATF.

Fig. 1 presents a diagram of the ATF. A ~15 ps FWHM bunch of electrons is produced by a laser photocathode electron gun and is accelerated to 70 MeV by two RF traveling-wave linac sections. The laser system consists of Nd:YAG and CO₂ lasers. The YAG laser serves as the linac photocathode driver and controls picosecond slicing in the CO₂ laser. The CO₂ laser beam is transported to several locations in the experimental hall where it interacts with electron bunches to test different laser acceleration schemes.

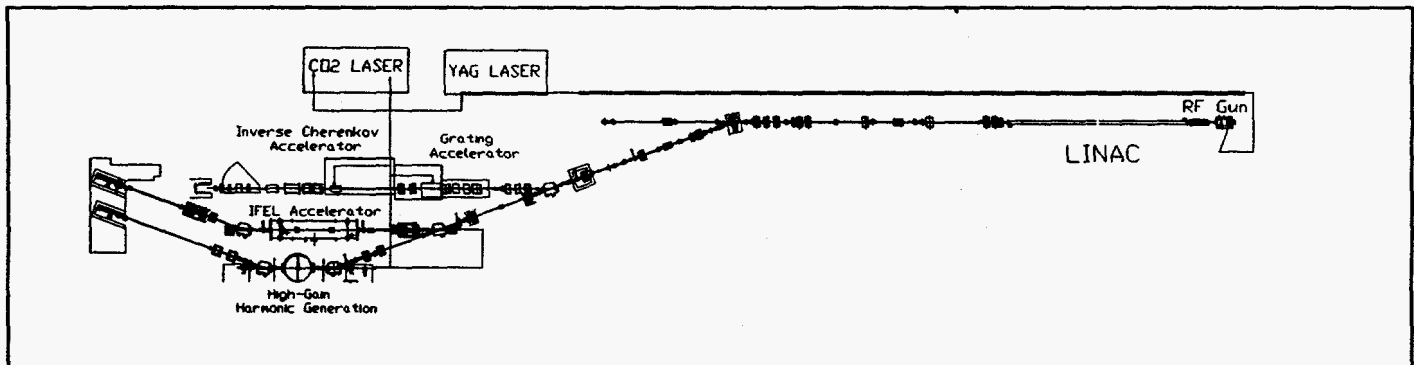


Fig. 1

Brookhaven Accelerator Test Facility

II. Nd:YAG Laser: Single-Pulse and Pulse Train Modes

The diagram in Fig. 2 shows the main subcomponents of the laser system and illustrates joint operation of the YAG and CO₂ lasers serving a laser acceleration experiment. An actively mode-locked CW YAG oscillator generates a train of 1 nJ, 12 ns spaced pulses of linearly polarized radiation synchronized with the linac RF field. A Pockels cell switch in combination with a polarizer cuts out single 15 ps FWHM pulses at a 3 Hz repetition rate. After a 4-pass preamplifier and a double-pass amplifier, pulses acquire 30 mJ of energy. Part of this energy is split to control picosecond slicing in the CO₂ system. The other portion is directed through second and, then, fourth harmonic crystals to a photocathode generating ~15 ps electron bunches.

Table 1 presents operational characteristics of the Nd:YAG laser. The application of a mode-locked laser as an RF gun driver puts exceptionally high requirements on the stability of all laser parameters. Instabilities larger than those specified in Table 1 would result in unacceptably high variations of accelerated electron energy, beam emittance, aberrations, etc. Such stringent requirements on stability are satisfied in part by using a Lightwave model 131 diode-pumped oscillator, which is characterized by appropriately small jitters in power and in mode-lock timing. Also, we use relay imaging and spatial filtering

*Work performed under the auspices of the U.S. Department of Energy, under contract
DE-AC02-76CH00016.

throughout the system, with long portions of beam path enclosed, including a 25 m vacuum tube for transport between the laser room and RF gun. Properly stabilized UV laser pulses are sent to the photocathode electron gun of the RF linac.

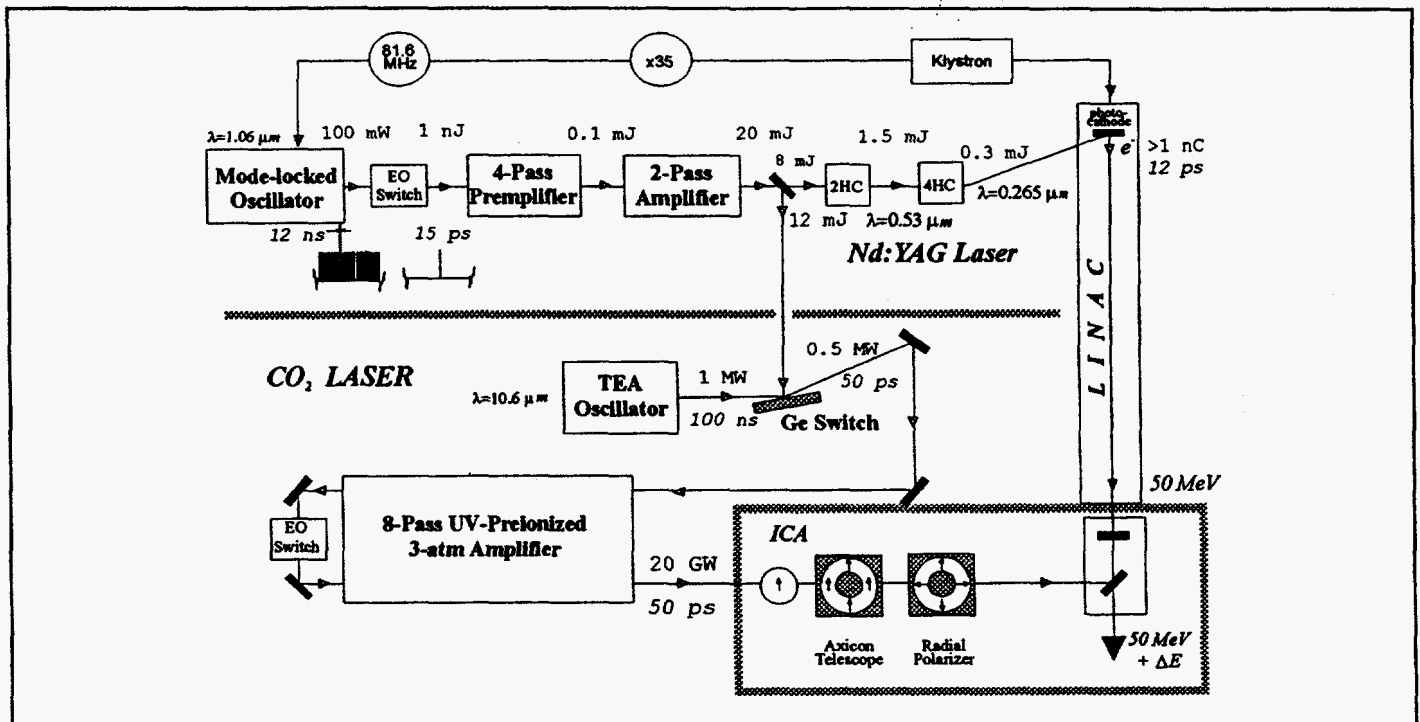


Fig.2
ATF laser system

ATF has a pioneering role in the development of photocathode RF guns for high-brightness electron accelerators. Fig.3 presents the configuration of the 3/2-cell RF gun used as an electron injector in the ATF linac. UV laser pulses of $\sim 50 \mu\text{J}$ energy are delivered to the Cu photocathode generating $\sim 15 \text{ ps}$ FWHM, $\sim 1 \text{ nC}$, electron bunches. To correct for ellipticity of the laser spot on the photocathode due to the oblique illumination, cylindrical lenses are used for beam focusing at the photocathode. To avoid phase-smearing, a stepped etalon will be used. High power (6 MW) S-band microwave pulse ($2.5 \mu\text{s}$) drives the gun to a high electric field (100 MV/m). The photoelectrons are accelerated to 4.5 MeV in the 8 cm long gun. Directly past the gun are the linac cavities where electrons are accelerated to 70 MeV with an energy spread of 0.4% rms and normalized emittance of $\sim 4\pi \text{ mm mrad}$.

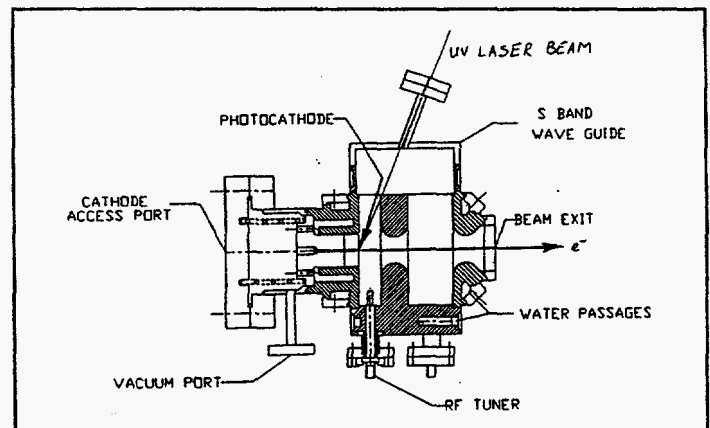


Fig.3
RF gun

So far, we have talked about producing single electron bunches with a repetition rate of 3 Hz. This regime, called single-pulse mode, is most regularly used during ATF operation (i.e., in laser acceleration experiments). But the ATF explores not just electron acceleration but also a free-electron lasers. For the visible FEL oscillator experiment, the linac should generate a train of electron bunches. Every electron bunch transmitted through the FEL wiggler generates photons. If the appropriate resonance and beam quality conditions are achieved, a build-up of coherent radiation is observed.

For this experiment, the YAG laser provides a square 3- μs train of laser pulses, 12 ns spaced, gated from the oscillator output with a Pockels cell switch. Since the requirement of the FEL experiment is a pulse train with a flat top, stable in amplitude to within 2%, this regime of operation presents an additional challenge: how to avoid natural energy drooping in the laser train due to gain depletion caused by the large extraction of energy throughout the pulse train. The solution is to

DISCLAIMER

Portions of this document may be illegible in electronic image products. Images are produced from the best available original document.

introduce an exponentially decreasing loss early in the amplification process. To accomplish this, another Pockels cell based amplitude controller is used to adjust the Nd:YAG preamplifier output. Transmission of this controller is modulated in time with an arbitrary waveform generator. Fig.4 shows test results of the amplitude control system. The first set of traces (a) is recorded with the control system off. We already observe energy droop after the preamplifier and more severe drop due to the gain depletion in the amplifier. Traces (b) show that, when the transmission through the preamplifier is properly adjusted in time, the central portion of the output train containing 200 pulses is stabilized within the requirements for the FEL experiment. The design parameters for the FEL experiment that is presently under way are presented in Table 2.

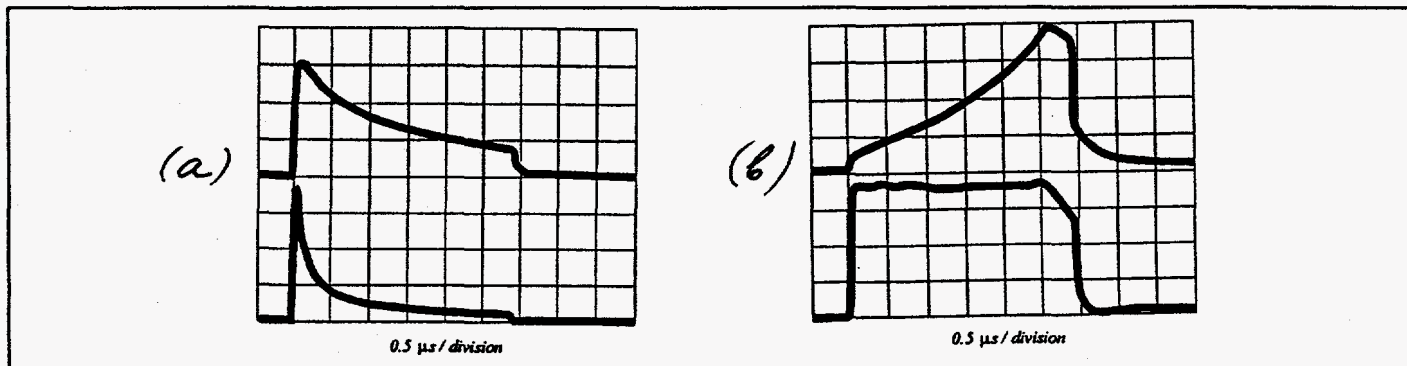


Fig.4

Pulse-train mode operation of the Nd:YAG laser; 1-preamplifier output envelope, 2- amplifier output envelope. (a) control system off, (b) control system on.

Table 1
Operational Characteristics of Nd:YAG Laser

Single pulse mode	
Total IR Energy [mJ]	30
IR Energy Split to CO2 Laser [mJ]	20
UV energy [mJ]	0.3
Pulse Duration FWHM [ps]	
Oscillator: IR	15
Amplifier: IR	25
UV pulse	12
Spot Size on Cathode [mm, $1/e^2 \text{ } \varnothing$]	0.1-1
Shot-to Shot Stability on Cathode	
Pulse Timing Jitter [ps]	<1
Pulse Duration Jitter [ps]	<1
Energy [%]	3
Pointing [% of beam diameter]	3
Pulse Train Mode	
Number of Pulses	200
Pulse Spacing [ns]	12
Energy per Micropulse (IR) [mJ]	1
Micropulse Energy Stability [%]	2

Table 2
Design Parameters for FEL Experiment

Electron Beam	
Energy [MeV]	48
Peak Current [A]	50
Microbunch Duration FWHM [ps]	15
Microbunch Rep. Rate [MHz]	40/81
Number of Microbunches	~200
Macrobunch Rep. Rate [Hz]	3
Undulator	
Period [cm]	0.88
Length [cm]	60
Gap [cm]	0.42
Peak Field (pulsed wiggler)[kG]	4.2
Laser Cavity	
Laser Wavelength [nm]	538
Cavity Length [cm]	367
Mirror Radius of Curvature [cm]	~200
Gain (per round trip) [%]	6.9
Outcoupling [%]	5
Output Power [MW]	10

III. Picosecond CO₂ Laser

The CO₂ laser, a block-diagram of which is presented in Fig.2, delivers high-power pulses of IR radiation synchronized with the electron bunches. Such synchronization is automatically achieved by optical switching of the CO₂ oscillator by the same YAG pulse which is ultimately used to drive the photocathode. Following the optical gating, the 1-MW oscillator pulse, now several picosecond long, is amplified to 20 GW peak power in 8 passes through a 1.2 m long 3-atm UV-preionized discharge.²

The hybrid single-longitudinal, zero-transverse mode TEA CO₂ oscillator is the source of the 10-μm beam. Single mode operation is provided by the combined use of a low-pressure auxiliary discharge, with a gain spectrum as narrow as the longitudinal mode separation, and piezo-electric fine tuning of the cavity length. The oscillator produces 100 ns, 1 MW laser pulses with a smooth envelope without mode-beating.

The semiconductor switching method is used to cut out a several picosecond pulse from the oscillator output. A YAG pulse, having a photon energy above the band gap of a semiconductor (Ge), creates an electron-hole plasma in a surface layer. When the plasma reaches a critical density, the refractive index becomes imaginary and Ge, which is normally transparent to 10-μm radiation, immediately turns into a total reflector. After the control pulse termination, the drop of reflection from the Ge has a characteristic time determined by the diffusion of the free-carriers into the bulk material, which is 150 ps. To define the trailing edge of the pulse and shorten it to a few picoseconds, the complement to reflection switching, transmission switching, is used for a second stage. In principle, the CO₂ pulse may be sliced as short as the electron bunch; that is ~12 ps. However, the lower limit on pulse duration is presently set by the amplifier bandwidth that depends upon the gas pressure. Presently, we use a 3-atm UV-preionized amplifier. The Fourier transform of its pressure broadened rotational spectrum gives 50 ps. That is the shortest pulse that we can efficiently amplify. After being amplified to 20 GW peak power, the 50-ps pulse is transported to the experimental hall where it is used for electron acceleration experiments.

IV. Laser Driven Electron Accelerator Experiments

The fundamental motivation for studying laser driven accelerators is the ultra-high electromagnetic fields attainable with high intensity pulsed lasers. For example., focusing of terawatt laser radiation results in intensities of the order of 10¹⁶ W/cm² and higher. The transverse electric field corresponding to such intensity is more than 300 GV/m. That is three orders of magnitude above the acceleration gradients produced by conventional electron accelerators. Various laser acceleration concepts involve conversion of a fraction of this enormous field into effective longitudinal accelerating field. We will talk about few of them that we are testing at the ATF.

One of them, the IFEL,³ illustrated by Fig.5, is based on the accelerating action of a linearly polarized laser beam on electrons having oscillating trajectories inside a wiggler magnet. The transverse laser field has an electric component along the local direction of the electron velocity. A pondermotive force produces an additional kick on the electrons in the direction of propagation if the laser field is in phase with wiggling. Synchronism conditions may be satisfied by adjusting the wiggler field and period. To ensure uniform acceleration over the 0.5 m length of the wiggler, the e-beam and CO₂ laser radiation will be channeled in a sapphire waveguide. Table 4 presents design parameters for the IFEL experiment. The full scale experiment requires 200 GW laser power, and the projected acceleration gradient is 90 MeV/m.

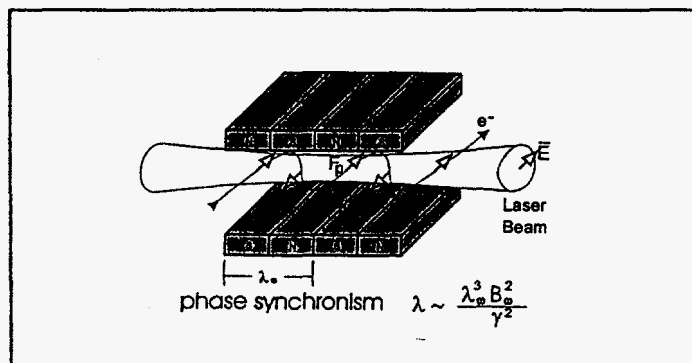


Fig.5
IFEL accelerator

Table 3
Operational Characteristics of CO₂ Laser

Oscillator Power [MW]	1
Oscillator Pulse Duration [ns]	100
Sliced Pulse Duration [ps]	30-300
Amplifier	
Repetition Rate [pulse/min]	3
Small Signal Gain [%/cm]	2.4
Saturation Fluence [mJ/cm ²]	25
Inverse Bandwidth [ps]	50
Amplified Pulse Duration [ps]	50
Peak Power [GW]	20

Table 4
Design Parameters for IFEL Experiment

Wiggler	
Length [cm]	47
Period [cm]	2.86-4.32
Gap [cm]	0.4
Field [T]	1.25
Electron Oscillation [mm]	0.17-0.22
CO ₂ Laser Driver	
Peak Power [GW]	200
Waveguide Losses [m ⁻¹]	0.025
Mean Accelerating Field [MV/m]	89

Another scheme called Grating Accelerator,⁴ illustrated by Fig.6, is based on excitation of an evanescent surface field when a laser beam is cylindrically focused onto a periodic structure. Electrons injected parallel to the surface will be accelerated when moving in phase with standing wave oscillations. This process is similar to what is observed in the RF linac, and is therefore also known as a Grating Linac. Operating parameters for this experiment are presented in Table 5. For a relativistic e-beam to satisfy the synchronism conditions, the structure period is nearly equal to the laser wavelength. Photographs of two possible structures produced by a lithographic etching technique are presented in Fig.7.

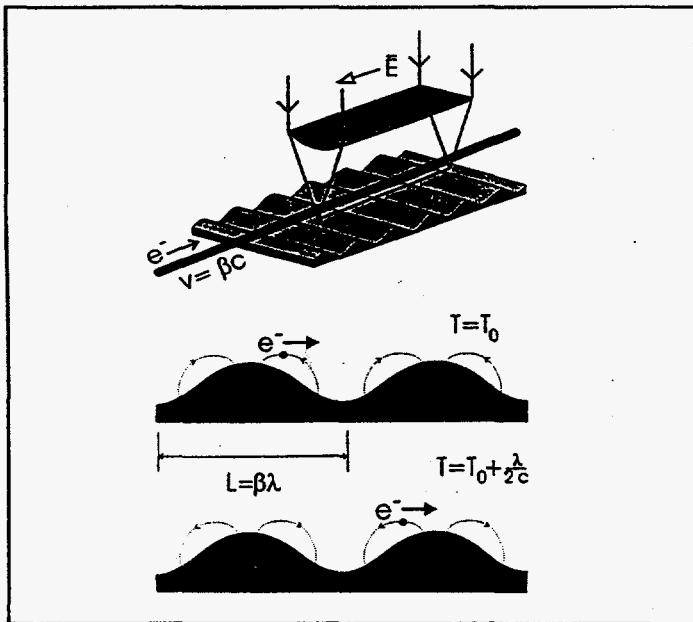


Fig.6
Grating Linac

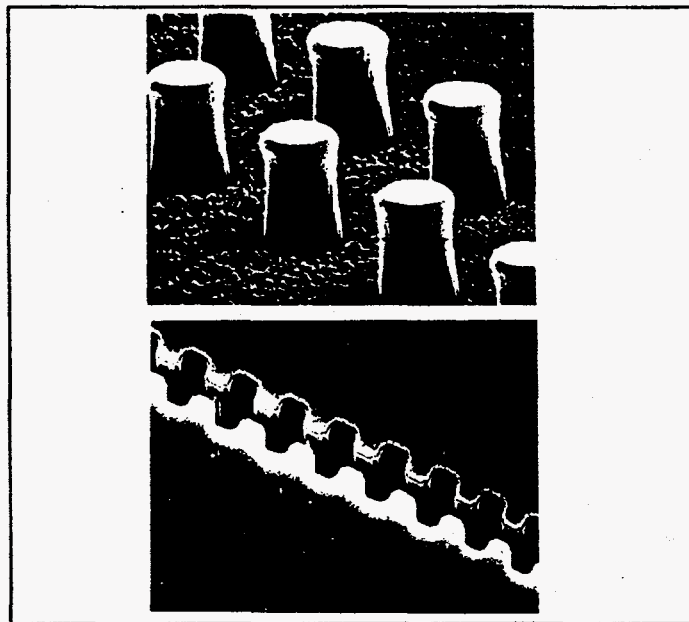


Fig.7
Grating Linac structures (period 10 μm)

In a third scheme shown in Fig.8, we start with a radially polarized laser beam. Using an axicon, the laser beam will be converged to the e-beam axis. Because of the wave-front inclination, a longitudinal component of the electric field will be developed. By filling the interaction cell with hydrogen, the phase-matching condition is satisfied, and the injected electron bunch propagates in phase with the optical field and experiences an acceleration. This process is opposite to coherent Cherenkov radiation. That is why this laser-driven electron acceleration scheme is called the Inverse Cherenkov Accelerator (ICA).^{5,6}

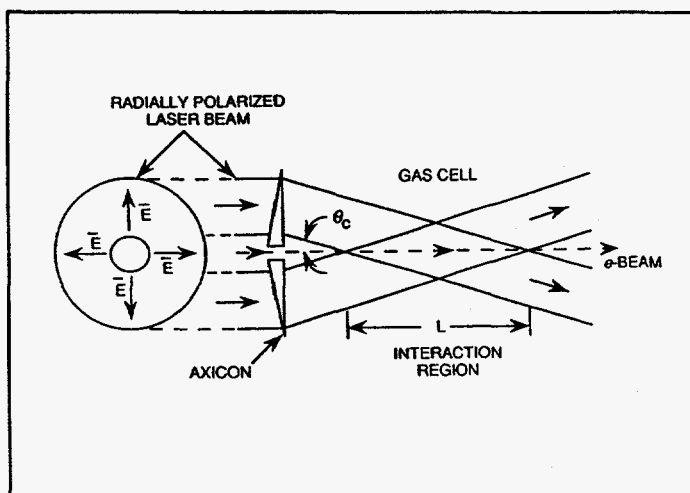


Fig.8
Axicon focusing in Inverse Cherenkov Accelerator

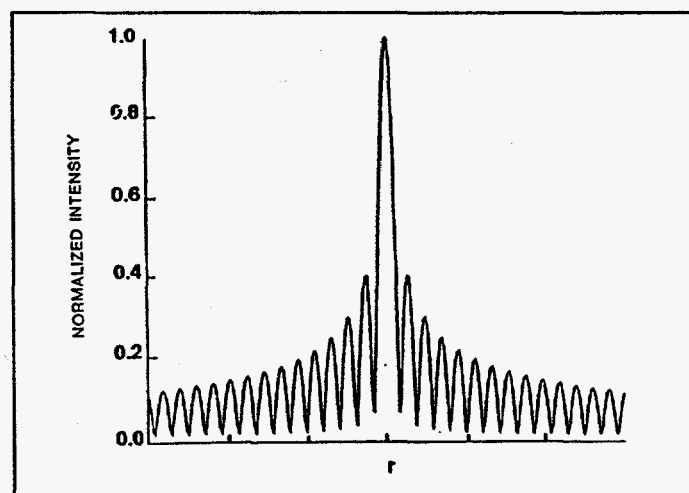


Fig.9
Longitudinal component of axicon-focused radial polarized laser beam

The radially polarized laser beam converged by the axicon produces a cylindrically symmetrical interference pattern. The longitudinal component of the electric field shown in Fig.9 has a maximum along the axis. The width of this maximum under the conditions of the ATF experiment is 400 μm , the same as the diameter of the e-beam.

In the first ICA run using a 0.7 GW CO_2 laser beam, up to 3.5 MeV peak acceleration has been observed.⁷ Up to 12 MeV acceleration over a 20 cm interaction distance is predicted by computer simulations for 5 GW of laser drive power.⁶ These figures are subject to experimental verification in the next ICA run.

Table 5
Design Parameters for Grating Linac

CO_2 Laser Power [GW]	1
Intensity [TW/cm^2]	0.3
Cylindrical Lens f-Number	5
Transverse Focus Size [μm]	50
Interaction Length [mm]	3
Electron Beam Radius [μm]	0.7
Accelerating Field [GV/m]	1.5

Table 6
Design Parameters for ICA Experiment

Cherenkov Angle [mrad]	20
Phase Matching Gas	H_2
Gas Pressure [atm]	1.7
Interaction Length [cm]	20
Electron Beam Diameter [mm]	0.2
Net Acceleration (@ 0.6 GW) [MeV]	3.7
Predicted Acceleration (@50 GW) [MeV]	36

V. 1 TW Picosecond CO_2 Laser Project

While 20 GW of available laser power is enough for the initial proof-of-principle experiments that are scheduled at the ATF, for more advanced experiments a much more powerful laser would be needed. For instance, the laser accelerator schemes described here are potentially scalable to 100 MeV. To reach this milestone, at least a 200 GW CO_2 laser will be required, which is 10 times more power than with the present laser. To meet these demands of advanced accelerators, the ATF is designing a modified CO_2 laser system approaching the Terawatt power level.⁸

Fig.10 presents the preferred configuration for the modified CO_2 laser system. The presently operational oscillator and picosecond pulse slicing system will supply a seed pulse into a regenerative preamplifier which may operate as a separate unit or may share a portion of the active discharge region in the final large-aperture amplifier that is preferably an X-ray preionized multi-atmosphere CO_2 laser. Three additional passes with beam expansion to $\sim 50 \text{ cm}^2$ will boost the output power to the 1 TW level. With a 10 ps pulse, this power corresponds to 10 J per pulse.

Table 7
Design Parameters for 1 TW CO_2 Laser

Preionization Source	x-ray
Repetition Rate [pulse/min]	5
Gas Pressure [atm]	5-10
Output Aperture [cm^2]	8×10
Discharge Length [cm]	100
Discharge Voltage [kV]	500
Energy Loading [$\text{J}/\text{l.atm}$]	120
Small Signal Gain [%/cm]	2.4
Saturation Fluence [mJ/cm^2]	500
Inverse Bandwidth [ps]	20
Rotational Relaxation Time [ps]	20
Output Pulse Duration [ps]	10
Output Fluence [mJ/cm^2]	200
Output Power [TW]	1

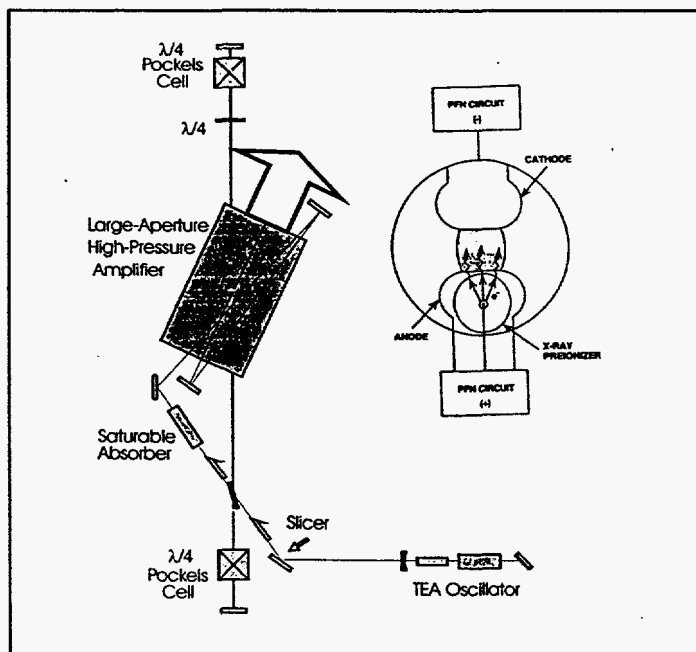


Fig.10
Terawatt CO_2 laser design

Acknowledgments

The authors wish to acknowledge the principal participants in the ATF experimental program for contributing data and valuable discussions, especially Arie van Steenbergen, Wayne Kimura, Rick Fernow and Palma Catravas. We also thank the staff of the ATF and NSLS for support in bringing much of the work described here to fruition. This work was performed under the auspices of the U.S. Department of Energy under Contract No. DE-AC02-76CH00016.

References

1. I. Ben-Zvi, in *Advanced Accelerator Concepts*, Port Jefferson, NY, 1992, AIP Conf. Proc., 279, 590 (1993).
2. I. Pogorelsky, J. Fischer, A.S. Fisher, T. Srinivasan-Rao, N.A. Kurnit, I.J. Bijio, R.F. Harrison, T. Shimada, Kusche, and M. Babzien, in *Lasers'93*, Lake Tahoe, NV, 1993, 647, (1994);
I.V. Pogorelsky, J. Fischer, K. Kusche, M. Babzien, N.A. Kurnit, I.J. Bijio, R.F. Harrison, and T. Shimada, *IEEE J. Quant. Electron.*, March, (1995) (to be published).
3. R.B. Palmer, *J. Appl. Phys.*, 43, 3014 (1972);
A. Fisher, J. Gallardo, J. Sandweiss, and A. van Steenbergen, in *Advanced Accelerator Concepts*, Port Jefferson, NY, 1992, AIP Conf. Proc., 279, 299 (1993).
4. R.B. Palmer, in *Laser Acceleration of Particles*, AIP Conf. Proc., 91, 179 (1982);
R.C. Fernow and J. Claus, in *Advanced Accelerator Concepts*, Port Jefferson, NY, 1992, AIP Conf. Proc., 279, 212 (1993).
5. J.R. Fontana and R.H. Pantell, *J. Appl. Phys.* 54, 4285 (1983).
6. R.D. Romea and W.D. Kimura, *Phys. Rev.*, 42D, 1807 (1990).
7. W.D. Kimura, G.H. Kim, R.D. Romea, L. Steinhauer, I.V. Pogorelsky, K.P. Kusche, R.C. Fernow, Xijie Wang, and Y. Liu, *Phys. Rev. Lett.*, May, (1994).
8. I.V. Pogorelsky, W.D. Kimura, C. Fisher, and N. Kurnit, in *Advanced Accelerator Concepts*, Fontana, WI, 1994, (to be published).

DISCLAIMER

This report was prepared as an account of work sponsored by an agency of the United States Government. Neither the United States Government nor any agency thereof, nor any of their employees, makes any warranty, express or implied, or assumes any legal liability or responsibility for the accuracy, completeness, or usefulness of any information, apparatus, product, or process disclosed, or represents that its use would not infringe privately owned rights. Reference herein to any specific commercial product, process, or service by trade name, trademark, manufacturer, or otherwise does not necessarily constitute or imply its endorsement, recommendation, or favoring by the United States Government or any agency thereof. The views and opinions of authors expressed herein do not necessarily state or reflect those of the United States Government or any agency thereof.